

DASH: Modularized Human Manipulation Simulation with Vision and Language for Embodied AI

Yifeng Jiang
Stanford University
United States of America
yifengj@stanford.edu

Michelle Guo
Stanford University
United States of America
mguo95@stanford.edu

Jiangshan Li
Stanford University
United States of America
jiangsli@stanford.edu

Ioannis Exarchos
Stanford University
United States of America
exarchos@stanford.edu

Jiajun Wu
Stanford University
United States of America
jiajunwu@cs.stanford.edu

C. Karen Liu
Stanford University
United States of America
karenliu@cs.stanford.edu

ABSTRACT

Creating virtual humans with embodied, human-like perceptual and actuation constraints has the promise to provide an integrated simulation platform for many scientific and engineering applications. We present Dynamic and Autonomous Simulated Human (DASH), an embodied virtual human that, given natural language commands, performs grasp-and-stack tasks in a physically-simulated cluttered environment solely using its own visual perception, proprioception, and touch, without requiring human motion data. By factoring the DASH system into a vision module, a language module, and manipulation modules of two skill categories, we can mix and match analytical and machine learning techniques for different modules so that DASH is able to not only perform randomly arranged tasks with a high success rate, but also do so under anthropomorphic constraints and with fluid and diverse motions. The modular design also favors analysis and extensibility to more complex manipulation skills.

CCS CONCEPTS

• **Computing methodologies** → **Modeling and simulation**; *Control methods*; *Machine learning*; **Animation**.

KEYWORDS

Virtual Human, Embodied AI System, Physics Simulation, Computer Vision, Reinforcement Learning.

ACM Reference Format:

Yifeng Jiang, Michelle Guo, Jiangshan Li, Ioannis Exarchos, Jiajun Wu, and C. Karen Liu. 2021. DASH: Modularized Human Manipulation Simulation with Vision and Language for Embodied AI. In *The ACM SIGGRAPH / Eurographics Symposium on Computer Animation (SCA '21)*, September 6–9, 2021, Virtual Event, USA. ACM, New York, NY, USA, 12 pages. <https://doi.org/10.1145/3475946.3480950>

Permission to make digital or hard copies of all or part of this work for personal or classroom use is granted without fee provided that copies are not made or distributed for profit or commercial advantage and that copies bear this notice and the full citation on the first page. Copyrights for components of this work owned by others than the author(s) must be honored. Abstracting with credit is permitted. To copy otherwise, or republish, to post on servers or to redistribute to lists, requires prior specific permission and/or a fee. Request permissions from permissions@acm.org.

SCA '21, September 6–9, 2021, Virtual Event, USA

© 2021 Copyright held by the owner/author(s). Publication rights licensed to ACM.
ACM ISBN 978-1-4503-8676-0/21/09...\$15.00
<https://doi.org/10.1145/3475946.3480950>

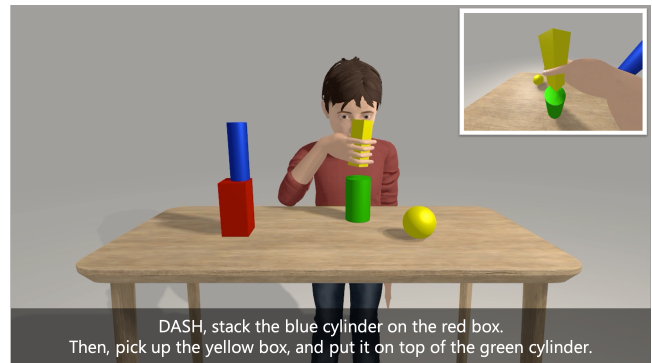


Figure 1: Our system, dynamic and autonomous simulated human (DASH), is an embodied virtual human modeled off of a child. DASH is able to manipulate tabletop objects with a dexterous arm and hand in a human-like way, using its own vision perception (white box), language understanding (user command in black box), proprioception and touch. (Video 0m12s)

1 INTRODUCTION

The recent breakthroughs in artificial intelligence (AI) have opened new avenues for computer graphics research [Chaudhuri et al. 2020; Peng et al. 2018; Tewari et al. 2020]. Systems originally built for graphics applications are also playing an increasingly important role in the progress of AI. For example, Embodied AI research, which centers around the idea that intelligence emerges from the inseparable interplay of sensorimotor activities and physical interactions with the environment [Smith and Gasser 2005], has utilized rendering systems and physics engines to provide inexpensive training data and testbeds. An integrated simulation environment with both realistic physics and visual appearances has the promise of creating diverse and safe playgrounds for virtual embodied AI agents to learn through interaction [Savva et al. 2019; Weihs et al. 2020; Xia et al. 2020].

In this paper, we argue for the crucial inclusion of simulated humans in Embodied AI systems using integrated techniques and knowledge from Computer Animation. Such virtual humans should not only manifest realistic physics and appearance, but also function autonomously under embodied anthropomorphic constraints,

such as egocentric vision, and with human-like interaction, such as natural language. Simulated humans that react to physics, perceive, and interact as real humans can provide an effective and safe platform for physical Human-Robot Interaction (pHRI) and assistive robotics, such as modeling human behavior during robot-assisted eating and drinking [Erickson et al. 2019]. Embodied virtual humans can also provide a new platform for scientific studies such as the perception-action coupling of infants' development: infants' initial physical interactions with the environment, though being imperfect with frequent failures, provide diverse experiences for perception development, which in turn facilitates motor skill learning. Though we envision most applications of our system to be in the virtual world, knowledge obtained through computational modeling of virtual humans could as well serve as a first step towards building physically embodied humanoid companions.

Such realistic modeling of human perception, actuation, and interaction constraints is in drastic contrast to existing virtual human systems, which either focus on visual appearance and motion realism [Antoniades 2016; Shapiro 2011], or on higher-level vision and language capabilities while abstracting out actual motor skills [Hartholt et al. 2013; Puig et al. 2018; Thiebaut et al. 2008]. In comparison with current cognitive modeling systems, such as the ACT-R [Anderson et al. 1997] simulator, which abstracts both perception and motor with symbolic modules, the physically embodied visual, verbal, and manual modules we aim to build could eventually be used to augment such systems. In contrast to existing character animation research, which usually does not simulate human perception, embodied virtual humans base their motor actions on noisy and partial perceptions of itself, rather than ground-truth simulator states.

To this end, we propose and build a system to physically simulate manipulation skills of a virtual human with egocentric vision, natural language command, proprioception, and touch—a first one to the best of our knowledge (Figure 1). We focus on object manipulation, which demands coordination between visual perception and motor dexterity. This system presents a unique set of requirements and challenges, as we summarize below:

- **Generality:** A highly generalizable system is crucial for our envisioned applications, because a simple verbal command alone could generate a wide variety of scenarios—our system must be capable of manipulating objects of different shapes and sizes arbitrarily placed in the workspace, while avoiding an unknown number of surrounding, arbitrarily arranged objects. Our system should demonstrate high success rates on a large number of such scenes.
- **Anthropomorphism:** We extend the conventional notion of “being humanlike” in character animation research to include both anthropomorphic constraints and humanlike behaviors. Our system should operate under anthropomorphic constraints such as delayed and noisy visual input. Our system must demonstrate fluid motion on a high degrees-of-freedom (DoF) anthropomorphic arm and hand, in contrast to slow, conservative motion optimized for functionality that is typically seen on robotic manipulation systems. As we opt to explore many humanlike constraints to be imposed on our system, this work does not aim to create motions of

better quality than current character animation techniques using full simulator states.

- **Extensibility:** Our system can be used as a self-contained black-box for Embodied AI research or pHRI. At the same, it should have sufficient modularity such that each module can be replaced or improved upon, so that more complex manipulation skills can be augmented to our first system without the need to redesign.
- **Interactivity:** The system should run at an interactive rate, allowing users to interact with the agent using online verbal commands.

Generality and anthropomorphism are often at odds with each other, because the demand of high success rates often results in a single conservative manipulation strategy with few natural variations. These important but sometimes conflicting goals prompt us to prioritize modularization in our system design. Specifically, we factor the problem into a vision module, a language module and manipulation modules for different stages, so that we can apply analytical methods to modules where correctness over a large range of scenarios are most important, and apply machine learning approaches to places where analytical methods are hard to solve and natural variations of motions are desired. As we are building a first system of its kind, modularization also facilitates analysis, interpretation, and extensibility.

We name our system Dynamic and Autonomous Simulated Human (DASH) and model DASH's visual appearance off a 5-year-old boy (Figure 1), as we believe modeling and understanding of the simultaneous acquisition of perceptual and motor skills are more important than demonstrating perfect skills themselves for embodied intelligence research. We evaluate the scenario in which DASH stands in front of a set of solid objects of various shapes and colors on a tabletop. The user gives DASH a sequence of grasp-and-stack commands in a domain-specific language to rearrange randomly scattered objects into a desired configuration. We evaluate the success rate of DASH accomplishing tasks correctly from randomized initial scenes, qualitatively demonstrate that DASH can produce fluid motions with natural variations, and analyze learned motor skills and various failure cases.

2 RELATED WORK

Virtual Human Systems. Creating virtual humans is a multidisciplinary research challenge in Computer Graphics, Artificial Intelligence, Cognitive Science, Human-Computer Interaction, and so forth. Many existing virtual human systems rely on pre-scripted, recorded or procedurally generated motion to animate the virtual humans in response to a set of predefined events [Caicedo and Thalmann 2000; Feng et al. 2014; Jung et al. 2011; Kalra et al. 1998; Magnenat-Thalmann and Egges 2006]. Multimodal dialog systems have demonstrated the use of virtual humans for verbal and non-verbal communication for training, education, and virtual assistant applications [Cassell et al. 2000; Chi et al. 2000; Lee and Marsella 2006; Matsuyama et al. 2016; Nguyen et al. 2015; Perera et al. 2018; Rickel and Johnson 1999]. Computational modelings of human cognition [Anderson et al. 1997; Funge et al. 1999] and perception mechanisms [Eom et al. 2019; Nakada et al. 2018; Peters and O'Sullivan 2002; Rabie and Terzopoulos 2000] have the promise of

not only creating realistic motions but also answering why humans show certain behaviors. Our work similarly models realistic human perceptual and physical constraints, but further directly utilizing RGB images and physics simulations as input. Our system generates human motion from computational models rather than motion data, allowing generalizable, unprescribed interactions with the world and potentially answering scientific questions.

Robotic Systems with Vision and Language. Systems that can perceive visual scenes and understand language instructions in a humanlike way have been explored both in simulations and on real-world robots. Virtual agents in [Puig et al. 2018; Shridhar et al. 2020] focus on high-level reasoning and abstracts motor skills with animated motion primitives, while our system focuses on fully physical motor skills. On real robots, similar manipulation systems [Hatori et al. 2018; Jiang et al. 2018; Liu and Zhang 2019; Mees et al. 2020; Paxton et al. 2019; Shridhar and Hsu 2018] usually employ robot grippers or suction cups where open-loop control primitives are robust enough for picking up objects. In contrast, this work explores the concatenation of multiple learned DRL controllers on a simulated anthropomorphic hand which produces more fluid and diverse motion while demonstrating robustness on precision tasks such as stacking of long and narrow objects.

Dexterous Manipulation in Computer Graphics. Dexterous manipulation is an integral component to creating interactive virtual humans. In Computer Graphics, previous works have proposed to generate physically plausible human grasps from recorded motion capture data [Pollard and Zordan 2005; Zhao et al. 2013], videos [Wang et al. 2013], or contact forces [Kry and Pai 2006], while our system aim at a more general grasp-and-stack task in a cluttered environment. Compared with other works [Andrews and Kry 2012; Liu 2009; Mordatch et al. 2012; Ye and Liu 2012] that animate dexterous manipulations, we rely on 2D images from the first-person view to infer estimated object information, without accessing contact point locations or forces from the ground-truth simulation states. A number of previous animation works also investigate the whole body motion during manipulation [Ho et al. 2010; Jain and Liu 2009; Lee et al. 2019; Yamane et al. 2004; Ye and Liu 2012]. Merel et al. [Merel et al. 2019, 2020] recently developed a hierarchical control framework that utilizes egocentric vision for locomotion and whole-body manipulation. Our work focuses on complex dexterous manipulation tasks in cluttered environments which requires coordinated planning with vision and language inputs, without requiring motion data.

Dexterous Manipulation in Robotics. In the Robotics community, manipulation primarily utilizes parallel jaw grippers, but dexterous hands have also been of great interest to researchers [Bicchi 2000; Ma and Dollar 2011; Okamura et al. 2000]. While we also solve grasping with dexterous hands, our system lift the requirement of grasp contact planning, facilitating the learned manipulation policies to zero-shot transfer to novel geometries. In recent years, researchers have begun to investigate DRL approaches for dexterous manipulation [Andrychowicz et al. 2020; Nagabandi et al. 2019; OpenAI et al. 2019]. Our work is most closely related to Radosavovic et al. [2020]; Rajeswaran et al. [2017], where they used a combination of policy learning and imitation learning to solve a

set of dexterous manipulation problems in simulation, including pick-and-place tasks. To reduce sample complexity and improve the quality of motion, Rajeswaran et al. [2017] used a VR system and CyberGlove system to capture high fidelity demonstrations from real humans. In contrast, our work does not require high-quality human demonstrations acquired by specialized equipment. In addition, our pick-and-place must be cognizant of other objects in the scene so the hand can avoid collisions or interact with them.

Computer Vision and Natural Language Processing. Recent development in deep learning has enabled perception systems that can directly learn scene representations from raw visual input, especially in constrained environments [Kulkarni et al. 2015; Mees et al. 2020; Nguyen-Phuoc et al. 2019; Sitzmann et al. 2019; Wu et al. 2017]. Directly related to our work, Yi et al. [2018] integrated an explicit visual representation with a language understanding module, leads to high accuracy on visual reasoning.

Semantic parsing algorithms learn to map sentences to logical forms via a knowledge base or a program [Berant et al. 2013; Guu et al. 2017; Liang et al. 2013]. Recently, Rothe et al. [2017] showed that formal programs can be effectively used to model human questions. For DASH, we choose to integrate an off-the-shelf learning-based semantic parser [Honnibal and Montani 2017] in our language module.

3 DASH: DYNAMIC AND AUTONOMOUS SIMULATED HUMAN

We mix and match analytical and learning approaches to balance between generality and anthropomorphism requirements, and to favor extensibility. As such, the DASH system consists of an ego-centric vision module, a language parsing module and manipulation modules of two skill categories: transition and interaction. We decompose the manipulation tasks in this work into four self-contained stages: reaching, grasping, transporting, and placing/stacking (Figure 2). We categorize reaching and transporting as transition stages, and grasping and placing/stacking as interaction stages. Here we discuss some key design decisions of our system.

Combined or independent vision and manipulation modules? We design a standalone vision module so we can reuse the same training procedure for different purposes (e.g. initial planning, stacking). Such modular design also allows us to activate or deactivate vision module independent of the manipulation module. Compared with having one end-to-end neural module, separating vision from motor training also significantly reduces time necessary for training anthropomorphic arms and hands with high degrees of freedom (DoFs). We also construct the vision architecture to be object-centric, meaning that the same trained model should be able to estimate properties of a varying number of objects in scene.

Integrated or skill-specific manipulation modules? Another design decision we made is to mix and match model-based planning and model-free reinforcement learning techniques for different manipulation stages. For transition stages (reaching, transporting), model-based planning has a probabilistic guarantee of a feasible solution if there exists one, agnostic to scene complexity; in contrast, learning a motor policy would require training to include all randomly arranged scenes, leading to a combinatorial explosion of

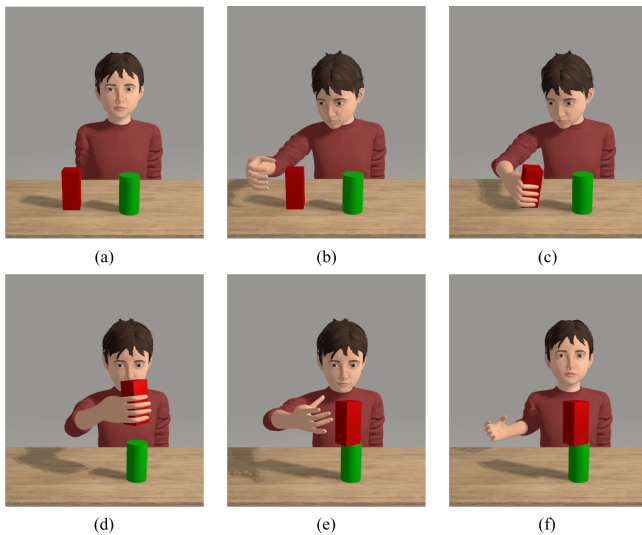


Figure 2: We break down the general pick-and-place task into stages. (a) initial rest pose; (b) end of reaching stage; (c) end of grasping stage; (d) end of transporting stage; (e) end of placing/stacking stage; (f) retract to task completion pose.

sample demand. On the other hand, using learned controllers for interaction stages produces more fluid and diverse motions compared to conservative open-loop grasping and placing primitives usually seen for robotic grippers, which often manifest one single strategy with sole finger motion and the arm fixed throughout. Concatenating multiple policies in one manipulation system strikes a balance between functionality and anthropomorphism, but it also poses additional challenges much unexplored in previous works, which we discuss in Section 3.4.

With or without human motion data? A final key design choice is avoiding the dependency on motion data. For our envisioned applications where scientific questions, such as how impacted perception affects motor skills, are asked, a system mimicking motion data from healthy actors will not be sufficient. Besides, since we are interested in a wide variety of highly constrained motion, such as stacking thin objects in a cluttered environment, imitation learning alone might not be able to produce feasible motions. On the other hand, we found that natural reaching motion can be achieved using model-based path planning with re-timing based on humanlike velocity profiles.

3.1 Vision Module

DASH includes a vision module that serves two main purposes: (i) to generate the scene observation for initial task planning and (ii) to provide frequent feedback to the manipulation module during object placing/stacking, both from raw RGB images. Our vision module consists of an object segmentation model and a feature extraction model, similar to [Yi et al. 2018]. Given a single scene image, the vision module first predicts segments for all objects in the scene. Each object segment is then concatenated with the original scene image and fed into a feature extraction network to output

attributes of this object, making the model agnostic to number of objects in the scene. The model predicts discrete attributes such as shape and color, as well as continuous attributes including height, 3D position, and upright axis for each object (full orientation is ambiguous for symmetrical objects). Gaze (head movement) is animated to match the decided camera locations during stages (i) and (ii), and interpolated between them for stages when vision module is turned off. Replacing head movement with eye movement where possible could benefit overall naturalness.

While our manipulation module can generalize to novel geometries unseen during training (Video 3m14s), zero-shot transfer is much more challenging for learning based vision algorithms. We therefore leave the generalization of vision beyond primitive shapes for future work. The generation of training data will be discussed in detail in Appendix A.1.

3.2 Language Module

The language module is invoked during initial task planning to infer the task parameters from the natural language command. We do not assume the specific form of the language command to allow natural variation in wording and ordering, as long as the command semantically specifies a target object to grasp, with reference object(s) and the desired final spatial relation to them. We assume both the target and reference objects can be modified by a shape, a color, and a modifier clause containing one secondary reference object and one secondary spatial relation for disambiguation.

Our language module consists of two steps: dependency parsing and parse tree search. We first use a robust neural-net-based dependency parser [Honnibal and Montani 2017] to obtain the semantic dependencies within our instruction sentence in the form of a tree. This step is general to any sentence structure. For the second step, with our assumptions, we perform a breadth-first search on the parse tree to identify the target object to grasp, the desired spatial relation defining the movement, and reference object(s).

The outputs of the vision and language modules are then cross-referenced. There might exist multiple objects sharing the same shape and color in the visual scene. A secondary search is performed in the clause subtree that modifies the target or reference object. The system will halt if the instruction still remains ambiguous after this disambiguation step. Coordinates of the target object location and the placing destination location are sent to the dexterous manipulation module.

3.3 Manipulation Module: Transition Stages

The transition stages (reaching and transporting) can be solved with model-based motion planning, using a common procedure agnostic to scene arrangement:

- (1) Compute the final arm pose that moves the hand close to target position for next stage, using the task parameters extracted by the vision and language modules;
- (2) Plan a collision-free trajectory for the arm and hand (with the object in-hand in case of transporting);
- (3) Execute the planned trajectory with close-loop tracking control.

For our system, instead of finding a single destination pose, we produce a distribution of destination poses, all of which have the

hand being close to the target position but with different palm facing orientations. Having multiple choices for the final pose increases the chance for the motion planner to yield a collision-free trajectory, alleviating failure cases where the destination arm configuration is already in collision. Moreover, the resultant motion exhibits richer diversity as the hand has multiple ways to approach the object. The distribution of poses are solved with a parameterized inverse kinematics (see Appendix A.2).

We solve for the collision-free trajectory with BiRRT algorithm [Kuffner and LaValle 2000], followed by shortening, smoothing [Hauser and Ng-Thow-Hing 2010], and re-timing (Appendix A.2) to eliminate robot-like disjunct motions. The re-timed trajectory is physically tracked with a PD control law and inverse dynamics.

3.4 Manipulation Module: Interaction Stages

We want to develop generic grasping and placing/stacking controllers capable of picking up objects of varying sizes, shapes, and locations, and placing objects on other objects or surfaces. We apply model-free deep reinforcement learning (DRL) to handle non-differentiable contacts involved, and fuse multiple sensory modalities of vision, proprioception, and touch. Our manipulation module can work without reasoning about grasping points, allowing it to zero-shot generalize to irregular object shapes unseen during training (Video 3m14s). We train one single grasping and one single placing/stacking policy by randomizing target object shapes and locations during training. Such randomization naturally leads the same policy to produce diverse behaviors.

Crucial to a successful concatenation of different stages, the initial distribution of arm and finger pose during policy training should adequately cover the space of possible scenarios that may result from its preceding stage. For both grasping and stacking stages, the initial arm poses are generated using the same procedure for generating final arm pose distributions during reaching and transporting. However, there is an additional difficulty in designing initial distribution for the stacking policy due to a unique challenge of multi-finger hand manipulation. With a dexterous hand, the relative transform between the hand and the object-in-hand has a considerable variance among different grasps. Thus, to learn a robust placing/stacking policy, we need to include such variance in the initial state distribution. As such, we use the grasping policy to collect 10,000 stable grasps, which we use to randomly initialize the hand pose and the configuration of the object-in-hand at the beginning of each training episode for the placing/stacking policy. Small white noise is injected to capture likely object slips during transportation.

Vision perception is crucial to placing/stacking, because this task requires updated feedback about the object configuration in the context of the scene. On the other hand, vision perception is less important for grasping as the reaching stage already leads the hand close to the object using the vision-estimated position from the initial scene. Thus, we use vision perception for placing/stacking and depend solely on proprioception and tactile perception during the grasping stage. Specifically, the observation space for the placing/stacking policy additionally includes the current 3D position and orientation of the involved objects as estimated by vision. For orientation, we only require the direction of the axis that indicates

the upright position of the object (for spheres we simply use a unit-z vector). To mimic the latency and low frequency of human visual perception system, we update the vision input at 20Hz and add 50 milliseconds of delay in the vision input to the policy. Since the training data of vision module is generated after the stacking policy is trained, during training of stacking we simply feed the policy with true object poses from simulation.

Technical details of the DRL modules are discussed in Appendix A.3.

4 EXPERIMENTS

In this section, we first evaluate whether the DASH system can balance between robustness and anthropomorphism, for which we both ‘stress test’ our system on 200 randomly generated trials and evaluate the success rates of the full system, and report qualitative evaluation on interactions with DASH. We also report the performance statistics of DASH.

We then conduct experiments on DASH’s vision module and manipulation module to evaluate our key system design decisions. We provide analysis on the accuracy of vision module, showing that a standalone vision module facilitates analysis and interpretation. We compare with the alternative design of a manipulation module, showing that merging all stages in one policy would cause difficulty in learning. We additionally show the zero-shot transfer capability of our manipulation module to objects with unseen, irregular shapes, showing the advantage of using close-loop, partially observable DRL policies which require no contact point reasoning. We finish this section with qualitative examples showing our manipulation module produces smooth motions with natural variation, and can be easily extended to manipulation with the left arm and hand.

4.1 Evaluations of the Whole System

We compare the system performance between using (i) ground truth object states (upper bound) and (ii) vision-predicted object attributes as the input observation to DASH using 200 randomly generated scenes (see Appendix B for details of setup). For ground truth evaluation, DASH is provided with perfect object attributes and 3D pose from the PyBullet simulator. For vision evaluation, DASH is provided with imperfect estimations of the objects.

Quantitative results. We show (Table 1) that DASH achieves high success rates on the large number of random scenes. We report two metrics of success: (i) success when considering all trials, and (ii) success when excluding trials that encountered a motion planning failure. A trial is considered successful if the (x, y) location of the placed object is within 10 cm of the target (x, y) , and the z coordinate of the center of mass is at least 5 cm above the target z coordinate. Success rates of DASH when using vision-estimated observations are within 5.8% of the success rates that use ground truth object states. Stacking success rates are generally around 10 to 15% lower than placing success rates, potentially due to higher sensitivity to observation accuracy.

We provide success rates excluding motion planning failures as additional reference since our randomly generated scenes and tasks

Table 1: Success rates (%) of the full system on 100 placing and 100 stacking tasks. We report success rates when (i) including all trials and (ii) excluding trials that fail due to motion planning (Figure 3). Vision denotes using imperfect estimations of object attributes from the vision module as input to DASH. Ground truth denotes perfect observation of object attributes. (Video 1m10s-1m35s)

Observation	All Trials			Excluding Plan Failures		
	Overall	Place	Stack	Overall	Place	Stack
Vision	76.0	82.0	70.0	85.8	89.1	82.4
Ground truth	79.0	83.0	75.0	89.7	91.2	88.2

may sometimes lead to motion planner unable to find a collision-free path during transition stages (Figure 3). Potential improvements could be training DASH to grasp from top of objects, and adding more Degrees of Freedoms (DoFs) around the shoulder complex. In summary, motion plan failures and stacking policy failures are the main sources of errors of our framework.

Qualitative results. To evaluate DASH’s motion quality, the accompanying video shows four successful examples of user-provided commands, mixing two-sentences and one-sentence commands with different kinds of modifiers (0m12s-1m10s). We wrote the instructions such that they cover the space specified by our assumptions (target object, reference object(s), at most one modifier clause), with variations in natural languages such as “stack on” vs “put on top of”. Example failure cases are also provided in the accompanying video (2m35s-3m02s).

Performance. Performance of the DASH system is measured on a personal desktop with Intel Core i7-9700K processor and The NVIDIA GeForce RTX 2080 Ti graphics card. The whole system runs at around 58 simulation steps per second. Rendering and communications between PyBullet and Unity contribute to a significant

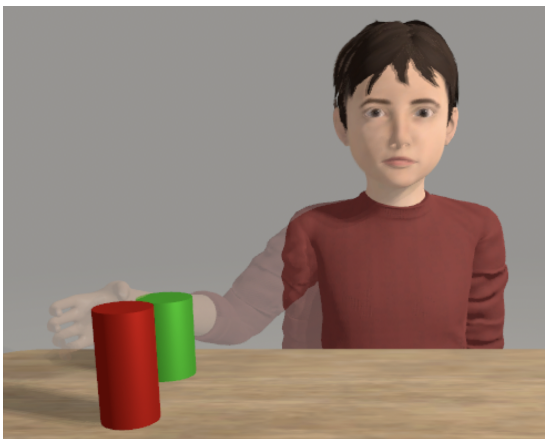


Figure 3: Motion planner during reaching stage unable to find a collision free path to destination arm pose shown in transparent.

Table 2: Vision module performance on the full system (test). We report classification accuracy on shape and color attributes, as well as the mean average error (MAE) on 3D position estimation (cm) across all predicted frames for the purpose of initial task planning, placing, or stacking. We show position prediction errors on all trials as well as when considering only successful trials.

Stage	Accuracy (%)		3D Position MAE (cm)	
	Shape	Color	All Trials	Successful Trials
Task Plan	100.0	100.0	(0.8, 1.1, 0.4)	(0.8, 1.3, 0.4)
Place	98.4	99.8	(3.8, 3.2, 2.3)	(2.8, 2.7, 1.8)
Stack	95.1	98.3	(3.5, 2.9, 2.6)	(2.7, 2.4, 1.9)

portion of the running time. Without Unity rendering, the manipulation module runs at around 360 simulation steps per second.

4.2 Analyses of the Vision Module

Having a stand-alone vision module allows us to analyze its performance independently. On the evaluation set (20% random split from the training data), as shown in Table 2, the vision module errors during initial task planning are much lower compared to the placing/stacking stage. This is likely due to the fact that DASH uses a fixed camera pose during planning, but varying camera pose to mimic human looking at destination during placing/stacking. In addition, DASH’s arm is not in the camera view during the planning stage. During the placing stage, DASH’s hand is in view, partially occluding the object in hand as well as surrounding objects, making pose estimation more challenging. Finally, during placing, the vision module and the policy interact in a tight feedback loop, resulting in potential compounding of errors over time. We also note that errors are generally lower when considering only successful trials instead of all trials. This suggests that the vision module could occasionally encounter states from failed placing attempts that are outside of its training distribution.

4.3 Analyses of the Manipulation Module

Comparison with learning-only approach. We show that stacking all four manipulation stages in one policy would cause problems in learning (Video 4m01s). The learning-only approach formulates the entire pick-and-place problem as a POMDP and solves for a single policy to achieve all four stages of the task: reaching, grasping, transporting and placing. In our attempt to train such a policy on a dexterous hand without any motion demonstration, we found that the state-of-the-art learning method fails at the very beginning of the task. It was unable to discover a collision-free path to move the arm from a resting (straight down) position to one that is above the tabletop. Subsequently, we significantly reduced the difficulty of the problem to a manipulation task commonly addressed by prior art. The simplified task only includes reaching and grasping, starting from a simple initial state where a clear collision-free path is available. With such simplification, we were able to successfully learn a policy using a learning-only approach, similar to the findings from previous work. But on a similar simplified task which includes reaching, grasping and stacking in place the training still fails. These

experiments confirm our hypothesis that a generic pick-and-place task “in the wild” can pose great challenges to a DRL approach, emphasizing the necessity of employing a hybrid approach of model-based planning and model-free learning.

Generalization to novel, non-primitive shapes. Without any re-training, we further demonstrate the grasp-and-stack task on non-primitive objects including an hourglass, a cone, and a Stanford bunny (Video 3m14s-3m40s). In these tasks we assume access to the object pose information without use of the vision module. Results show that our policy generalizes to novel, irregularly shaped geometries for the pick-and-place task.

Emergent behaviors with natural variations. Since both our grasping and placing policies are required to handle a large range of task variation during training, multiple behaviors naturally emerge from the same grasping or placing policy (Video 1m40s-2m16s). For instance, the grasping policy occasionally rotates the target object slightly in order to execute a more stable grasp. In other cases, if an object is unstable and close to falling over during the grasping processes, the policy may switch to grasping the bottom of the object as a rescue strategy. Similar variation of behaviors can be observed for the placing/stacking policy as well. During placing or stacking, if the object in hand is in an upright orientation, the policy may choose to simply release the object from midair and allow the object to drop onto the placing surface. In other scenarios, the policy may choose to be conservative and wait for the object placing to finish before releasing its hand. If a placed object appears to be on the verge of falling over, the hand often maintains contact with object in an effort to restabilize it.

Effect of reshaping and retiming. We show in the accompanying video (2m22s) that our reshaping and retiming technique (Figure 5) creates more smooth reaching motions, compared with directly using the trajectory solved by the robotics package OpenRave. A comparison of the palm velocity profiles is also given in Figure 4.

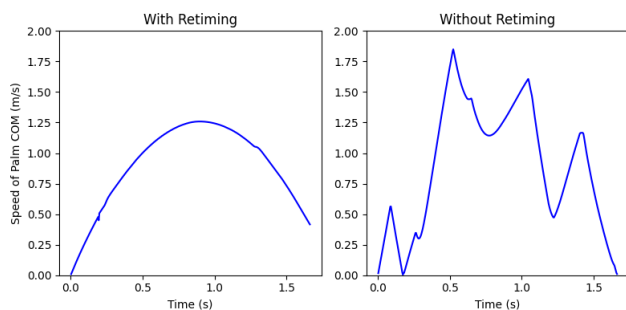


Figure 4: Velocity profiles of the palm during reaching to object, with our retiming/reshaping technique, or using the OpenRave solved trajectory without editing.

Extension: dual-arm manipulation. In the accompanying video (3m45s), we show that the same policies trained for the right arm can be directly mirrored and used for the left arm.

5 DISCUSSION AND CONCLUSION

This paper introduces DASH, a first system for simulating human manipulation skills with humanlike embodied constraints and language interaction. We show that it is possible to build an embodied virtual human that solely uses its own visual perception, natural language parsing, proprioception, and touch to perform grasp-and-stack tasks in a physically-simulated, cluttered environment. By factoring the DASH system into a vision module, a language module and manipulation modules of two skill categories, we are able to mix and match analytical and machine learning techniques for different modules, so that DASH is able to not only perform randomly arranged tasks with a high success rate, but also does so under incomplete information and with fluid and diverse motions.

Our system does not depend on recorded human motion, hence having the potential to be used for both engineering applications such as physical human-robot interaction, and scientific applications such as the cognitive modeling of how embodied constraints affect human motions. By carefully concatenating DRL manipulation policies, our system can work without reasoning about grasping points, allowing it to zero-shot generalize to irregular object shapes unseen during training.

As the focus of the DASH system is to explore the inclusion of various humanlike constraints, we are not able to use certain existing techniques to improve motion quality, such as grasping algorithms that utilize explicit geometry and contact point analysis. That said, the motion quality of the current version of DASH can be much improved by allowing the torso to move and adding more DoFs at the shoulder complex. This will also enlarge the reachable area [Rodriguez et al. 2003], and could help the inverse kinematics solver to avoid finding poses with large wrist bending.

There are many possible choices for the vision module design. We choose egocentric RGB vision as it is closer to the human vision system. Alternative designs such as third-person point clouds reconstructed from dual cameras could have made the system easier to build. More scientific knowledge can be injected to the vision module to make it more humanlike. For example, the location uncertainty of human vision is not only distance dependent, but also depends on nearby reference objects including the reaching hand.

DASH is currently limited to grasping and placing/stacking tasks, but the modular design facilitates extensions such as concatenating additional DRL policies for more complex skills. Just as humans simultaneously learn perception and motor skills, interleaving stacking and vision training (instead of only once in the current system) could further improve the robustness of the system.

Even though the use of partially-observable DRL policies allows our manipulation module to transfer easily to unseen shapes, achieving the same transfer for vision module is much more challenging. One future direction is to train the vision module with a large set of everyday objects, randomly arranged on the tabletop. Finally, while our language module is robust to some wording (e.g. “put on” versus “stack it on”) and natural ordering variations, it will not handle ambiguous commands. This can be addressed by allowing DASH to ask domain-specific questions when instructions are ambiguous.

ACKNOWLEDGMENTS

The authors would like to thank Michael Hayashi for mirroring the trained policies for the dual-arm setting.

REFERENCES

- John R Anderson, Michael Matessa, and Christian Lebiere. 1997. ACT-R: A theory of higher level cognition and its relation to visual attention. *Human-Computer Interaction* 12, 4 (1997), 439–462.
- Sheldon Andrews and Paul G. Kry. 2012. Policies for Goal Directed Multi-Finger Manipulation. In *Workshop on Virtual Reality Interaction and Physical Simulation*, Jan Bender, Arjan Kuijper, Dieter W. Fellner, and Eric Guerin (Eds.). The Eurographics Association. <https://doi.org/10.2312/PE/vrphys/vrphys12/137-145>
- Marcin Andrychowicz, Bowen Baker, Maciek Chociej, Rafal Jozefowicz, Bob McGrew, Jakub Pachocki, Arthur Petron, Matthias Plappert, Glenn Powell, Alex Ray, et al. 2020. Learning dexterous in-hand manipulation. *The International Journal of Robotics Research* 39, 1 (2020), 3–20.
- Tameem Antoniades. 2016. Creating a Live Real-Time Performance-Captured Digital Human. In *ACM SIGGRAPH 2016 Real-Time Live!* (Anaheim, California) (SIGGRAPH '16). Association for Computing Machinery, New York, NY, USA, Article 36, 1 page. <https://doi.org/10.1145/2933540.2933551>
- Jonathan Berant, Andrew Chou, Roy Frostig, and Percy Liang. 2013. Semantic parsing on freebase from question-answer pairs. In *Proceedings of the 2013 conference on empirical methods in natural language processing (EMNLP)*. 1533–1544.
- Antonio Bicchi. 2000. Hands for dexterous manipulation and robust grasping: A difficult road toward simplicity. *IEEE Transactions on robotics and automation* 16, 6 (2000), 652–662.
- Samuel R Buss. 2004. Introduction to inverse kinematics with jacobian transpose, pseudoinverse and damped least squares methods. *IEEE Journal of Robotics and Automation* 17, 1-19 (2004), 16.
- Angela Caicedo and Daniel Thalmann. 2000. *Virtual Humanoids: Let them be autonomous without losing control*. Technical Report. Swiss Federal Institute of Technology, EPFL.
- Justine Cassell, Joseph Sullivan, Elizabeth Churchill, and Scott Prevost. 2000. *Embodied conversational agents*. MIT press.
- Siddhartha Chaudhuri, Daniel Ritchie, Jiajun Wu, Kai Xu, and Hao Zhang. 2020. Learning generative models of 3D structures. In *Computer Graphics Forum*, Vol. 39. Wiley Online Library, 643–666.
- Diane Chi, Monica Costa, Liwei Zhao, and Norman Badler. 2000. The EMOTE Model for Effort and Shape. In *Proceedings of the 27th Annual Conference on Computer Graphics and Interactive Techniques (SIGGRAPH '00)*. ACM Press/Addison-Wesley Publishing Co., USA, 173–182.
- Erwin Coumans and Yunfei Bai. 2016–2019. PyBullet, a Python module for physics simulation for games, robotics and machine learning. <http://pybullet.org>.
- Rosen Diankov. 2010. *Automated Construction of Robotic Manipulation Programs*. Ph.D. Dissertation. Carnegie Mellon University, Robotics Institute.
- Haegwang Eom, Daseong Han, Joseph S Shin, and Junyong Noh. 2019. Model Predictive Control with a Visuomotor System for Physics-based Character Animation. *ACM Transactions on Graphics (TOG)* 39, 1 (2019), 1–11.
- Zackory Erickson, Vamsee Gangaram, Ariel Kapusta, C Karen Liu, and Charles C Kemp. 2019. Assistive Gym: A Physics Simulation Framework for Assistive Robotics. *arXiv preprint arXiv:1910.04700* (2019).
- Andrew Feng, Yazhou Huang, Yuyu Xu, and Ari Shapiro. 2014. Fast, automatic character animation pipelines. *Computer Animation and Virtual Worlds* 25, 1 (2014), 3–16.
- John Funge, Xiaoyuan Tu, and Demetri Terzopoulos. 1999. Cognitive modeling: knowledge, reasoning and planning for intelligent characters. In *Proceedings of the 26th annual conference on Computer graphics and interactive techniques*. 29–38.
- Ross Girshick, Ilija Radosavovic, Georgia Gkioxari, Piotr Dollár, and Kaiming He. 2018. Detectron. <https://github.com/facebookresearch/detectron>
- Kelvin Guu, Panupong Pasupat, Evan Liu, and Percy Liang. 2017. From Language to Programs: Bridging Reinforcement Learning and Maximum Marginal Likelihood. In *Proceedings of the 55th Annual Meeting of the Association for Computational Linguistics (ACL)*. 1051–1062.
- Arno Hartholt, David Traum, Stacy C Marsella, Ari Shapiro, Giota Stratou, Anton Leuski, Louis-Philippe Morency, and Jonathan Gratch. 2013. All together now. In *International Workshop on Intelligent Virtual Agents*. Springer, 368–381.
- Jun Hatori, Yuta Kikuchi, Sosuke Kobayashi, Kuniyuki Takahashi, Yuta Tsuboi, Yuya Unno, Wilson Ko, and Jethro Tan. 2018. Interactively picking real-world objects with unconstrained spoken language instructions. In *2018 IEEE International Conference on Robotics and Automation (ICRA)*. IEEE, 3774–3781.
- Kris Hauser and Victor Ng-Thow-Hing. 2010. Fast smoothing of manipulator trajectories using optimal bounded-acceleration shortcuts. In *2010 IEEE international conference on robotics and automation*. IEEE, 2493–2498.
- Kaiming He, Georgia Gkioxari, Piotr Dollár, and Ross Girshick. 2017. Mask r-cnn. In *Proceedings of the IEEE international conference on computer vision*. 2961–2969.
- Kaiming He, Xiangyu Zhang, Shaoqing Ren, and Jian Sun. 2016. Deep residual learning for image recognition. In *Proceedings of the IEEE conference on computer vision and pattern recognition*. 770–778.
- Edmond S. L. Ho, Taku Komura, and Chiew-Lan Tai. 2010. Spatial Relationship Preserving Character Motion Adaptation. *ACM Trans. Graph.* 29, 4, Article 33 (2010), 8 pages.
- Matthew Honnibal and Ines Montani. 2017. spaCy 2: Natural language understanding with Bloom embeddings, convolutional neural networks and incremental parsing. (2017).
- Sumit Jain and C. Karen Liu. 2009. Interactive Synthesis of Human-Object Interaction. In *Proceedings of the 2009 ACM SIGGRAPH/Eurographics Symposium on Computer Animation (New Orleans, Louisiana) (SCA '09)*. Association for Computing Machinery, New York, NY, USA, 47–53.
- Yuqian Jiang, Shiqi Zhang, Piyush Khandelwal, and Peter Stone. 2018. Task Planning in Robotics: An Empirical Comparison of PDDL-based and ASP-based Systems. *arXiv preprint arXiv:1804.08229* (2018).
- Yvonne Jung, Arjan Kuijper, Dieter W. Fellner, Michael Kipp, Jan Miksatko, Jonathan Gratch, and Daniel Thalmann. 2011. Believable Virtual Characters in Human-Computer Dialogs. In *Eurographics 2011 - State of the Art Reports*, N. John and B. Wyvill (Eds.). The Eurographics Association.
- Prem Kalra, Nadia Magnenat-Thalmann, Laurent Moccozet, Gael Sannier, Amaury Aubel, and Daniel Thalmann. 1998. Real-time animation of realistic virtual humans. *IEEE Computer Graphics and Applications* 18, 5 (1998), 42–56.
- Eliyahu Kiperwasser and Yoav Goldberg. 2016. Simple and accurate dependency parsing using bidirectional LSTM feature representations. *Transactions of the Association for Computational Linguistics* 4 (2016), 313–327.
- Sujatha Krishnan-Barman, Paul AG Forbes, and Antonia F de C Hamilton. 2017. How can the study of action kinematics inform our understanding of human social interaction? *Neuropsychologia* 105 (2017), 101–110.
- Paul G. Kry and Dinesh K. Pai. 2006. Interaction capture and synthesis. *ACM Trans. Graph.* 25, 3 (2006), 872–880.
- James J Kuffner and Steven M LaValle. 2000. RRT-connect: An efficient approach to single-query path planning. In *Proceedings 2000 ICRA. Millennium Conference. IEEE International Conference on Robotics and Automation. Symposia Proceedings (Cat. No. 00CH37065)*, Vol. 2. IEEE, 995–1001.
- Harold W Kuhn. 1955. The Hungarian method for the assignment problem. *Naval research logistics quarterly* 2, 1-2 (1955), 83–97.
- Tejas D Kulkarni, William F Whitney, Pushmeet Kohli, and Joshua B Tenenbaum. 2015. Deep convolutional inverse graphics network. In *Advances in neural information processing systems (NeurIPS)*. 2539–2547.
- Jina Lee and Stacy Marsella. 2006. Nonverbal Behavior Generator for Embodied Conversational Agents. In *Proceedings of the 6th International Conference on Intelligent Virtual Agents (Marina Del Rey, CA) (IVA'06)*. Springer-Verlag, Berlin, Heidelberg, 243–255.
- Seunghwan Lee, Moonseok Park, Kyoungmin Lee, and Jehee Lee. 2019. Scalable Muscle-Actuated Human Simulation and Control. *ACM Trans. Graph.* 38, 4, Article 73 (July 2019), 13 pages.
- Percy Liang, Michael I Jordan, and Dan Klein. 2013. Learning dependency-based compositional semantics. *Computational Linguistics* 39, 2 (2013), 389–446.
- Tsung-Yi Lin, Piotr Dollár, Ross Girshick, Kaiming He, Bharath Hariharan, and Serge Belongie. 2017. Feature pyramid networks for object detection. In *Proceedings of the IEEE conference on computer vision and pattern recognition*. 2117–2125.
- C. Karen Liu. 2009. Dexterous Manipulation from a Grasping Pose. In *ACM SIGGRAPH 2009 Papers (New Orleans, Louisiana) (SIGGRAPH '09)*. Association for Computing Machinery, New York, NY, USA, Article 59, 6 pages.
- Rui Liu and Xiaoli Zhang. 2019. A review of methodologies for natural-language-facilitated human-robot cooperation. *International Journal of Advanced Robotic Systems* 16, 3 (2019), 1729881419851402.
- Raymond R Ma and Aaron M Dollar. 2011. On dexterity and dexterous manipulation. In *2011 15th International Conference on Advanced Robotics (ICAR)*. IEEE, 1–7.
- Nadia Magnenat-Thalmann and Arjan Egges. 2006. Interactive virtual humans in real-time virtual environments. *IJVR* 5, 2 (2006), 15–24.
- Yoichi Matsuyama, Arjun Bhardwaj, Ran Zhao, Oscar Romeo, Sushma Akjoju, and Justine Cassell. 2016. Socially-aware animated intelligent personal assistant agent. In *Proceedings of the 17th annual meeting of the special interest group on discourse and dialogue*. 224–227.
- Oier Mees, Alp Emek, Johan Vertens, and Wolfram Burgard. 2020. Learning Object Placements for Relational Instructions by Hallucinating Scene Representations. *arXiv preprint arXiv:2001.08481* (2020).
- Josh Merel, Saran Tunyasuvunakool, Arun Ahuja, Yuval Tassa, Leonard Hasenclever, Vu Pham, Tom Erez, Greg Wayne, and Nicolas Heess. 2019. Reusable neural skill embeddings for vision-guided whole body movement and object manipulation. *arXiv preprint arXiv:1911.06636* (2019).
- Josh Merel, Saran Tunyasuvunakool, Arun Ahuja, Yuval Tassa, Leonard Hasenclever, Vu Pham, Tom Erez, Greg Wayne, and Nicolas Heess. 2020. Catch and Carry: Reusable Neural Controllers for Vision-guided Whole-Body Tasks. *ACM Trans. Graph.* 39 (July 2020).

- Hamza Merzić, Miroslav Bogdanović, Daniel Kappler, Ludovic Righetti, and Jeannette Bohg. 2019. Leveraging contact forces for learning to grasp. In *2019 International Conference on Robotics and Automation (ICRA)*. IEEE, 3615–3621.
- Igor Mordatch, Zoran Popović, and Emanuel Todorov. 2012. Contact-Invariant Optimization for Hand Manipulation. In *Proceedings of the ACM SIGGRAPH/Eurographics Symposium on Computer Animation (Lausanne, Switzerland) (SCA '12)*. Eurographics Association, Goslar, DEU, 137–144.
- Anusha Nagabandi, Kurt Konogle, Sergey Levine, and Vikash Kumar. 2019. Deep Dynamics Models for Learning Dexterous Manipulation. *arXiv preprint arXiv:1909.11652* (2019).
- Masaki Nakada, Tao Zhou, Honglin Chen, Tomer Weiss, and Demetri Terzopoulos. 2018. Deep Learning of Biomimetic Sensorimotor Control for Biomechanical Human Animation. *ACM Trans. Graph.* 37, 4, Article 56 (July 2018), 15 pages.
- Truong-Huy D Nguyen, Elin Carstensdottir, Nhi Ngo, Magy Seif El-Nasr, Matt Gray, Derek Isaacowitz, and David Desteno. 2015. Modeling warmth and competence in virtual characters. In *International Conference on Intelligent Virtual Agents*. Springer, 167–180.
- Thu Nguyen-Phuoc, Chuan Li, Lucas Theis, Christian Richardt, and Yong-Liang Yang. 2019. Hologan: Unsupervised learning of 3d representations from natural images. In *Proceedings of the IEEE International Conference on Computer Vision (ICCV)*. 7588–7597.
- Allison M Okamura, Niels Smaby, and Mark R Cutkosky. 2000. An overview of dexterous manipulation. In *Proceedings 2000 ICRA. Millennium Conference. IEEE International Conference on Robotics and Automation. Symposia Proceedings (Cat. No. 00CH37065)*, Vol. 1. IEEE, 255–262.
- OpenAI, Ilge Akkaya, Marcin Andrychowicz, Maciek Chociej, Mateusz Litwin, Bob McGrew, Arthur Petron, Alex Paino, Matthias Plappert, Glenn Powell, Raphael Ribas, et al. 2019. Solving Rubik's Cube with a Robot Hand. *arXiv preprint arXiv:1910.07113* (2019).
- Chris Paxton, Yonatan Bisk, Jesse Thomason, Arunkumar Byravan, and Dieter Fox. 2019. Propection: Interpretable plans from language by predicting the future. In *2019 International Conference on Robotics and Automation (ICRA)*. IEEE, 6942–6948.
- Xue Bin Peng, Angjoo Kanazawa, Jitendra Malik, Pieter Abbeel, and Sergey Levine. 2018. SFV: Reinforcement Learning of Physical Skills from Videos. *ACM Trans. Graph.* 37, 6, Article 178 (Nov. 2018), 14 pages.
- Ian Perera, James Allen, Choh Man Teng, and Lucian Galescu. 2018. Building and learning structures in a situated blocks world through deep language understanding. In *Proceedings of the First International Workshop on Spatial Language Understanding*. 12–20.
- Christopher Peters and Carol O'Sullivan. 2002. Synthetic vision and memory for autonomous virtual humans. In *Computer Graphics Forum*, Vol. 21. Wiley Online Library, 743–752.
- Nancy S. Pollard and Victor Brian Zordan. 2005. Physically Based Grasping Control from Example. In *Proceedings of the 2005 ACM SIGGRAPH/Eurographics Symposium on Computer Animation (Los Angeles, California) (SCA '05)*. Association for Computing Machinery, New York, NY, USA, 311–318.
- Xavier Puig, Kevin Ra, Marko Boben, Jiaman Li, Tingwu Wang, Sanja Fidler, and Antonio Torralba. 2018. Virtualhome: Simulating household activities via programs. In *Proceedings of the IEEE Conference on Computer Vision and Pattern Recognition*. 8494–8502.
- Tamer F Rabie and Demetri Terzopoulos. 2000. Active perception in virtual humans. In *Vision Interface*, Vol. 2000.
- Ilija Radosavovic, Xiaolong Wang, Lerrel Pinto, and Jitendra Malik. 2020. State-Only Imitation Learning for Dexterous Manipulation. *arXiv preprint arXiv:2004.04650* (2020).
- Aravind Rajeswaran, Vikash Kumar, Abhishek Gupta, Giulia Vezzani, John Schulman, Emanuel Todorov, and Sergey Levine. 2017. Learning complex dexterous manipulation with deep reinforcement learning and demonstrations. *arXiv preprint arXiv:1709.10087* (2017).
- Jeff Rickel and W Lewis Johnson. 1999. Animated agents for procedural training in virtual reality: Perception, cognition, and motor control. *Applied artificial intelligence* 13, 4-5 (1999), 343–382.
- I Rodriguez, Manuel Peinado, Ronan Boulic, and Daniel Meziat. 2003. Bringing the human arm reachable space to a virtual environment for its analysis. In *2003 International Conference on Multimedia and Expo. ICME '03. Proceedings (Cat. No. 03TH8698)*, Vol. 1. IEEE, 1–229.
- Anselm Rothe, Brenden M Lake, and Todd Gureckis. 2017. Question asking as program generation. In *Advances in neural information processing systems (NeurIPS)*. 1046–1055.
- Manolis Savva, Abhishek Kadian, Oleksandr Maksymets, Yili Zhao, Erik Wijmans, Bhavana Jain, Julian Straub, Jia Liu, Vladlen Koltun, Jitendra Malik, et al. 2019. Habitat: A platform for embodied ai research. In *Proceedings of the IEEE International Conference on Computer Vision*. 9339–9347.
- John Schulman, Filip Wolski, Prafulla Dhariwal, Alec Radford, and Oleg Klimov. 2017. Proximal policy optimization algorithms. *arXiv preprint arXiv:1707.06347* (2017).
- Ari Shapiro. 2011. Building a character animation system. In *International conference on motion in games*. Springer, 98–109.
- Mohit Shridhar and David Hsu. 2018. Interactive visual grounding of referring expressions for human-robot interaction. *arXiv preprint arXiv:1806.03831* (2018).
- Mohit Shridhar, Jesse Thomason, Daniel Gordon, Yonatan Bisk, Winson Han, Roozbeh Mottaghi, Luke Zettlemoyer, and Dieter Fox. 2020. Alfred: A benchmark for interpreting grounded instructions for everyday tasks. In *Proceedings of the IEEE/CVF Conference on Computer Vision and Pattern Recognition*. 10740–10749.
- Vincent Sitzmann, Michael Zollhöfer, and Gordon Wetzstein. 2019. Scene representation networks: Continuous 3D-structure-aware neural scene representations. In *Advances in Neural Information Processing Systems (NeurIPS)*. 1119–1130.
- Linda Smith and Michael Gasser. 2005. The development of embodied cognition: Six lessons from babies. *Artificial life* 11, 1-2 (2005), 13–29.
- Ayush Tewari, Ohad Fried, Justus Thies, Vincent Sitzmann, Stephen Lombardi, Kalyan Sunkavalli, Ricardo Martin-Brualla, Tomas Simon, Jason Saragih, Matthias Nießner, Rohit Pandey, Sean Fanello, Gordon Wetzstein, Jun-Yan Zhu, Christian Theobalt, Maneesh Agrawala, Eli Shechtman, Dan B. Goldman, and Michael Zollhöfer. 2020. State of the Art on Neural Rendering. *Computer Graphics Forum* (2020). <https://doi.org/10.1111/cgf.14022>
- Marcus Thiebaut, Stacy Marsella, Andrew N Marshall, and Marcelo Kallmann. 2008. Smartbody: Behavior realization for embodied conversational agents. In *Proceedings of the 7th international joint conference on Autonomous agents and multiagent systems-Volume 1*. 151–158.
- Yangang Wang, Jianyuan Min, Jianjie Zhang, Yebin Liu, Feng Xu, Qionghai Dai, and Jinxiang Chai. 2013. Video-Based Hand Manipulation Capture through Composite Motion Control. *ACM Trans. Graph.* 32, 4, Article 43 (July 2013), 14 pages.
- Luca Weihs, Jordi Salvador, Klemen Kotar, Unnat Jain, Kuo-Hao Zeng, Roozbeh Mottaghi, and Aniruddha Kembhavi. 2020. AllenAct: A Framework for Embodied AI Research. *arXiv* (2020).
- Jiajun Wu, Joshua B Tenenbaum, and Pushmeet Kohli. 2017. Neural scene de-rendering. In *Proceedings of the IEEE Conference on Computer Vision and Pattern Recognition (CVPR)*. 699–707.
- Fei Xia, William B Shen, Chengshu Li, Priya Kasimbeg, Micael Edmond Tchappmi, Alexander Toshev, Roberto Martin-Martin, and Silvio Savarese. 2020. Interactive Gibson Benchmark: A Benchmark for Interactive Navigation in Cluttered Environments. *IEEE Robotics and Automation Letters* 5, 2 (2020), 713–720.
- Katsu Yamane, James J. Kuffner, and Jessica K. Hodgins. 2004. Synthesizing Animations of Human Manipulation Tasks. In *ACM SIGGRAPH 2004 Papers* (Los Angeles, California) (SIGGRAPH '04). Association for Computing Machinery, New York, NY, USA, 532–539.
- Yuting Ye and C. Karen Liu. 2012. Synthesis of Detailed Hand Manipulations Using Contact Sampling. *ACM Trans. Graph.* 31, 4, Article 41 (July 2012), 10 pages.
- KeXin Yi, Jiajun Wu, Chuang Gan, Antonio Torralba, Pushmeet Kohli, and Joshua B Tenenbaum. 2018. Neural-symbolic vqa: Disentangling reasoning from vision and language understanding. In *Advances in Neural Information Processing Systems (NeurIPS)*. 1031–1042.
- Wenping Zhao, Jianjie Zhang, Jianyuan Min, and Jinxiang Chai. 2013. Robust Realtime Physics-Based Motion Control for Human Grasping. *ACM Trans. Graph.* 32, 6, Article 207 (Nov. 2013), 12 pages.

A SYSTEM IMPLEMENTATIONS

In this section we present additional technical material that is important to the success of the DASH system.

A.1 Vision and Language Modules

A.1.1 Vision module. We use Mask R-CNN [He et al. 2017] with a ResNet-50 FPN [Lin et al. 2017] backbone as our segmentation model, implemented using the “Detectron” library [Girshick et al. 2018]. The model is trained for 100K iterations with a batch size of two and learning rate of 2.5×10^{-4} . For our feature extraction model, we train a ResNet-18 [He et al. 2016] for each of the planning, placing, and stacking stages for 60K iterations using a learning rate of 0.002 and batch size of 20. The model inputs are resized to 480 by 480.

The model is trained in camera coordinates; at test time, the predictions from the vision module are transformed from the camera coordinate frame into the world coordinate frame using the camera pose. We then use the Kuhn-Munkres (Hungarian) algorithm [Kuhn 1955] to associate objects predicted across time, based on their predicted attributes.

We use the Unity 3D game engine¹ to render training images and object segmentations. The camera is placed near the eyes of DASH to provide vision observation. At the initial task planning (before manipulation starts), the DASH camera points at a fixed location such that the camera view covers the main region that manipulable objects lie. The information predicted from this first image is used to generate a task plan jointly with language module. During placing/stacking stage, the camera points at the destination x, y location predicted during task planning. The camera target locations during training are computed using ground truth object locations with 2 centimeter noise for robustness.

The vision module is trained on frames from both the initial tabletop scene and the placing stage to serve its two usages. We generate 20K training images of initial tabletop scenes following the same procedure as that of our full system evaluation pipeline (see Appendix B). To generate examples from the placing stage, we collect 4,000 rollouts from a pretrained placing/stacking policy. For this step of data generation, the policy utilizes perfect object pose information from simulator, with an additional 2 centimeter noise on object positions and 0.03 noise on up vectors. From all frames generated from the policy rollouts, we uniformly downsample 40K frames for vision training.

A.1.2 Language module. We used the neural network based dependency parser proposed by Kiperwasser and Goldberg [2016] which is robust to noise in natural language, and its open source implementation in spaCy [Honnibal and Montani 2017]. For the breadth-first search, we pre-define a dictionary of shape, color, and spatial relation keywords. There might exist multiple objects sharing same shape and color in the visual scene. To disambiguate, we then search in the subtrees of the target object and of the primary reference object token for secondary spatial relations and secondary reference object(s) that modify the target or reference object.

¹Unity game engine website: <https://unity3d.com/>

A.2 Manipulation Module: Transition Stages

The manipulation controller operates on an anthropomorphic arm and hand including four fingers, a thumb, and a palm, totaling 29 degrees of freedom. For clarity of exposition, we will refer the degrees of freedom (dofs) from the shoulder to the palm as $\mathbf{q}^A \in \mathbb{R}^7$ and the dofs for finger joints as $\mathbf{q}^F \in \mathbb{R}^{22}$. We only simulate and control DASH’s right arm and right hand in main experiments, but also show that the same manipulation controller can be easily mirrored to the left arm and hand. We use the PyBullet physics engine [Coumans and Bai 2019] as the simulator.

A.2.1 Compute the final arm pose. From the initial image of the scene and the language instruction, the vision and language modules jointly infer the high-level pick-and-place task parameters, including the index of the target object, its initial position $\bar{\mathbf{p}}_i \in \mathbb{R}^3$, its desired position $\bar{\mathbf{p}}_d \in \mathbb{R}^3$, and estimated initial locations and shapes of all objects in the scene. Our first goal is to find the final arm pose $\bar{\mathbf{q}}_T^A$ such that the palm is close to the initial position $\bar{\mathbf{p}}_i$ at the end of the reaching stage, and close to the desired position $\bar{\mathbf{p}}_d$ at the end of the transporting stage.

To solve a distribution of final poses for the arm, we consider an Inverse Kinematics (IK) problem that matches the position and orientation of the palm in the world frame to a desired affine transformation T , parameterized by a random variable θ ,

$$T(\theta) = \begin{bmatrix} \mathbf{R}_z(\theta) & \mathbf{p} \\ 0 & 1 \end{bmatrix} T_0, \quad (1)$$

where \mathbf{p} is assigned to the initial or desired position $\bar{\mathbf{p}}_i$ or $\bar{\mathbf{p}}_d$ depending on the stage, $\mathbf{R}_z(\theta)$ is a rotation matrix about z-axis (upright axis) by angle θ , and T_0 is a constant transformation from the object frame to the palm frame, manually designed for each task. For example, for the reaching stage, T_0 positions the right palm at 20cm to the right of the object, with the palm facing the object. We uniformly sample $\theta \in [0, 2\pi]$ to create multiple candidates for the final arm pose. The implication is that we can grasp and hold the object from multiple orientations by its side, but not from its top. This multiple candidate IK problem is iterated by candidate and each solved with [Buss 2004]. The selected final arm pose $\bar{\mathbf{q}}_T^A$ is a collision-free pose with the wrist closest to its rest angle.

A.2.2 Plan a collision-free trajectory. Once the final arm pose $\bar{\mathbf{q}}_T^A$ is determined, the next task is to plan a smooth trajectory for the arm and the hand from the initial pose given by the previous stage (for the first reaching stage we simply use the rest pose) to $\bar{\mathbf{q}}_T^A$, while avoiding collision with objects in the scene.

There exist many efficient and reliable motion planning algorithms from robotics literature. We apply BiRRT [Kuffner and LaValle 2000] to first search for a collision-free path and then shorten and smoothen the path using techniques proposed by [Hauser and Ng-Thow-Hing 2010]. We use the open-source implementation in OpenRave [Diankov 2010] to obtain a collision-free trajectory $\bar{\mathbf{q}}_{1:T}^A$.

The trajectory solved by OpenRave assumes zero terminal palm velocity since this is the usual convention in robotics systems. While this is fine for the transition between transporting and stacking, complete stop of palm at the switching from reaching to grasping would result in unnatural, robot-like motions. As OpenRave does not control the direction of the terminal tangent (because of zero

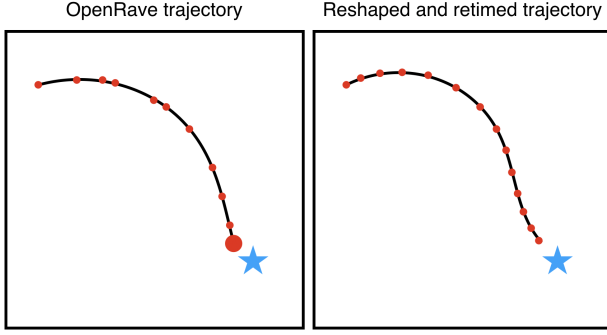


Figure 5: Illustration: Reaching trajectory of the arm/palm solved from OpenRave is reshaped and retimed to have non-zero velocity before the grasping motion starts, making the stage switching more natural.

terminal speed), we first reshape the OpenRave trajectory by replacing the final 10% with a Hermite curve, so that the terminal tangent points from the palm towards the object; then a retiming is performed on the edited trajectory to fit a quadratic velocity profile, mimicking that human arm first accelerates then decelerates during reaching [Krishnan-Barman et al. 2017]. We set the terminal palm speed to 0.4m/s. Figure 5 shows an illustration of this procedure.

The finger joints trajectory $\bar{\mathbf{q}}_{1:T}^F$ holds the same manually designed pose in Figure 2 (b) throughout reaching, and the same grasping pose (see next paragraph) throughout transporting. During planning, we replace the hand (and the object-in-hand) with a conservative bounding box to speed up the computation.

A.2.3 Simulate the planned trajectory. To track the planned trajectory $\bar{\mathbf{q}}_{1:T}^A$ in a physics simulation, we first compute the desired velocity $\dot{\mathbf{q}}^+$ in the next time step using a PD control law,

$$\dot{\mathbf{q}}^+ = -K_p(\mathbf{q}_t - \bar{\mathbf{q}}_t) - (K_d - 1)\dot{\mathbf{q}}_t, \quad (2)$$

where \mathbf{q}_t and $\dot{\mathbf{q}}_t$ are the joint state at current time step. The desired velocity is realized by solving for the appropriate control torque via Inverse Dynamics, and then sending solved torques to joint motors for forward simulation in Bullet. Note that $\dot{\mathbf{q}}^+$ is not always achieved due to joint limits, torque limits, and the presence of environment contacts. The stability of simulation is not sensitive to the gains K_p and damping coefficients K_d , as a result of solving torque from Inverse Dynamics.

During the transporting stage, we must ensure that the grasped object does not fall out of the hand. Since the contact force applied to the object is due to the tracking error of the hand pose, the target hand pose should be designed in a way such that it induces effective forces to secure the object and is unachievable during the transporting phase (so the hand will continuously apply contact force to the object). Instead of manually designing such a pose, we use the sign of the tracking error in the last time step during the grasping stage, $\mathbf{e} = \text{sign}(\bar{\mathbf{q}}_g^F - \mathbf{q}_g^F)$, to define the target pose during transporting as $\bar{\mathbf{q}}_{tran}^F = \mathbf{q}_g^F + 0.1\mathbf{e}$.

A.3 Manipulation Module: Interaction Stages

We train a policy $\pi(\mathbf{a}_t|\mathbf{o}_t)$ that maps the agent’s current observation \mathbf{o}_t to its action \mathbf{a}_t every $k = 6$ simulation steps. We formulate the problem of grasping and placing or stacking objects as a Partially-Observable Markov Decision Process $(\mathcal{S}, \mathcal{O}, \mathcal{A}, f, r, p_0, g, \gamma)$, where \mathcal{S} is the state space, \mathcal{O} is the observation space, \mathcal{A} is the action space, $f(\cdot)$ is the system dynamics, $r(\cdot)$ is the reward function, $g(\cdot)$ is the observation function, p_0 is the initial state distribution, and γ is the discount factor. We use a policy gradient method, PPO [Schulman et al. 2017], to solve for a policy π such that the accumulated reward is maximized:

$$J(\pi) = \mathbb{E}_{s_0, a_0, \dots, s_T} \sum_{t=0}^T \gamma^t r(s_t, a_t), \quad (3)$$

where $s_0 \sim p_0$, $a_t \sim \pi(a_t|\mathbf{o}_t)$, $\mathbf{o}_t \sim g(s_t)$ and $s_{t+1} = f(s_t, a_t)$. Unlike model-based motion planning, reinforcement learning requires offline training of the policy. While the observations will be partial and noisy, we assume during training the reward function additionally has access to the complete, accurate simulator state s_t to better evaluate training progress.

A.3.1 Observation space and action space. The observation space contains information from proprioception and tactile sensors, as well as information about the task. The stacking policy additionally uses frequent vision module estimates, as discussed in Section 3.4.

The proprioception consists of the current state and the target pose from the previous time step: $(\mathbf{q}_t, \dot{\mathbf{q}}_t^A, \bar{\mathbf{q}}_{t-1})$. Empirically, we found that finger velocity $\dot{\mathbf{q}}_t^F$ does not improve performance, and its wide range and sensitivity to contacts hurts generalization. The tactile perception on the hand is represented as a vector of binary numbers c_t , each of which denotes whether the corresponding phalanx is in contact with an object. The task information contains the location of interaction, i.e., $\bar{\mathbf{p}}_i$ for grasping and $\bar{\mathbf{p}}_d$ for placing/stacking, and a one-hot vector representing the shape of the object (e.g., cylinder, box, or sphere) to grasp, place, or stack.

The action space is defined as the change in desired joint angles $\Delta\bar{\mathbf{q}}$ from the previous time step. Using the same velocity-based control scheme described in Appendix A.2, we compute the required torque so that the finger joints can closely track $\dot{\mathbf{q}}_t = \dot{\bar{\mathbf{q}}}_{t-1} + \Delta\dot{\bar{\mathbf{q}}}$.

A.3.2 Initial state distribution. At the beginning of each rollout during training, we sample from the initial state distribution p_0 to reset the scene containing the arm, hand and involved objects, from which the agent starts a new trial of grasping or placing/stacking. Our goal is to design p_0 such that it covers the space of possible scenarios that may result from its preceding stage. As such, p_0 first provides randomization over the involved object’s shape, size, mass, and friction coefficient, sampled from uniform distributions with ranges listed in Appendix B. We also sample $\bar{\mathbf{p}}_i$ or $\bar{\mathbf{p}}_d$ uniformly to cover the reachable range of the arm. We apply white noise within 2 cm to the sampled $\bar{\mathbf{p}}$ and use it to reset the involved object’s initial position. The additional white noise prepares the policy to handle vision inaccuracy of $\bar{\mathbf{p}}$ from initial task planning. With the updated $\bar{\mathbf{p}}_i$ or $\bar{\mathbf{p}}_d$, we follow the procedure described in Section A.2 to generate a set of arm poses parameterized by θ .

A.3.3 Reward function design for grasping. Empirically, we found that the more variation in the initial state distribution that our

policies are required to handle, the more carefully we need to design the reward function in order to help policy training avoid undesired local optima. The reward function of our grasping policy at each step $r_t^G(\mathbf{s}_t, \mathbf{a}_t)$ consists of the following terms (all norm operators $\|\cdot\|$ below denote Euclidean distance):

$$r_t^G = 10r_t^o + r_t^p + 2r_t^c + 1.5r_t^s + r_t^d, \quad (4)$$

each of which we will elaborate below.

The object pose term r_t^o discourages objects from moving too much horizontally, which might lead to knocking over surrounding objects during test time:

$$r_t^o = -\|(\mathbf{p}_t - \bar{\mathbf{p}}_i)_{x,y}\|, \quad (5)$$

where \mathbf{p}_t is the object location provided by the simulator and the subscript (x, y) indicates that the height difference is ignored.

Let $\mathbf{h}_1(\mathbf{q}^F), \dots, \mathbf{h}_5(\mathbf{q}^F)$ be the world locations of the finger tips from the thumb to the little finger, and $\mathbf{h}_p(\mathbf{q}^F)$ be the world location of the palm. The form closure term r_t^p encourages five finger tips and the palm to stay close to the object:

$$r_t^p = -5\|\mathbf{h}_{1,t} - \mathbf{p}_t\| - \sum_{i=2}^5\|\mathbf{h}_{i,t} - \mathbf{p}_t\| - 2\|\mathbf{h}_{p,t} - \mathbf{p}_t\|. \quad (6)$$

The contact term $r_t^c = |\mathbf{c}|$ encourages more phalanxes to be in contact with the object. Similarly to Equation 6, we weigh the thumb contact five times more than other fingers.

The finger shaping term r_t^s encourages the four fingers to have a similar pose:

$$r_t^s = -\|\mathbf{q}^{F2} - \mathbf{q}^{F3}\| - \|\mathbf{q}^{F3} - \mathbf{q}^{F4}\| - \|\mathbf{q}^{F4} - \mathbf{q}^{F5}\| - \|\mathbf{q}^{F5} - \mathbf{q}^{F2}\|, \quad (7)$$

where $\mathbf{q}^{F2}, \dots, \mathbf{q}^{F5}$ are the subsets of \mathbf{q}^F that correspond to the four finger DOFs.

Finally, similar to the training scheme used in Merzić et al. [2019], we add a ‘drop test’ around the end of each training episode to increase robustness of the policy. During the test, we remove the table and apply downward external forces on the object for around 0.4s. We add a penalty $r_t^d = -15$ for each control step during this test if the object is dropped. Designing a reward function that encourages lifting behaviors can be done by rewarding force closure or terminal height of the object, but we found that directly altering the physics environment results in more sample-efficient learning.

A.3.4 Reward function design for placing and stacking. Designing the reward function for the placing and stacking policy is more challenging as success states are sparse and the dynamics are much less stable. At each step the reward $r_t^P(\mathbf{s}_t, \mathbf{a}_t)$ consists of the following terms:

$$r_t^P = 5r_t^o + 10r_t^a - 0.5r_t^c + 0.3r_t^s + r_t^b. \quad (8)$$

With a slight abuse of notation, the object pose term r_t^o for placing penalizes both position and orientation deviations from a desired object final pose $\bar{\mathbf{p}}_f$, where the object-in-hand is in an upright pose above the bottom object or at the correct location on the tabletop:

$$r_t^o = -\|\mathbf{p}_t - \bar{\mathbf{p}}_f\| + 3\mathbf{z}^T \mathbf{R}_t \mathbf{z}, \quad (9)$$

where \mathbf{p}_t is the position of the object being placed, \mathbf{R}_t is its rotation matrix, and $\mathbf{z} = [0, 0, 1]$, the direction of gravity.

The action sparsity term r_t^a encourages sparse hand force during placing. Since in our PD-like control scheme, the source of hand force is the tracking error $\bar{\mathbf{q}} - \mathbf{q}$, r_t^a is defined as:

$$r_t^a = 1/(\|\bar{\mathbf{q}} - \mathbf{q}_t\| + 1). \quad (10)$$

We use the same definition of contact term r_c and the finger shaping term r_s as in those defined for grasping. Instead of encouraging contact with the object ($2r_c$), we slightly discourage ($-0.5r_c$) it during placing/stacking.

Finally, a bonus term $r_t^b = 5$ is added for each step *if* the object-in-hand is sufficiently close to $\bar{\mathbf{p}}_f$, and an additional bonus $r_t^b = 20$ is added *if* the hand releases object when the object is close to $\bar{\mathbf{p}}_f$.

A.3.5 Training details. We use the default learning parameters reported in the original PPO algorithm [Schulman et al. 2017] to train both the grasping and placing/stacking policies. We train the grasping policy for 12M simulation steps and placing/stacking for 16M simulation steps. To train one single policy that could both stack an object and place it on tabletop, we randomly split 70% of the training episodes for stacking trials and 30% for placing. Since stacking spheres is unlikely to be successfully trained, we trained a separate sphere grasping policy and placing-on-table policy for qualitative demonstrations only.

B QUANTITATIVE EVALUATION SETUP

We randomly generate 200 scenes and tasks to systematically assess the generality of our system. For each scene, the task is randomly selected from either (i) place an object at a specified (x, y, z) location, or (ii) stack an object on top of another object. Language is excluded from this experiment, as random commands generated by a program is effectively the same as randomly sampled the parameters of pick-and-stack tasks. We leave user studies with natural language commands provided by users to future work.

For each object in the scene, we randomly sample shape (box, cylinder, or sphere), color (red, yellow, green, or blue), width ($[6, 10]$ cm), height ($[13, 18]$ cm), base position ($-0.1 \leq x \leq 0.25$, $-0.1 \leq y \leq 0.5$, $z = 0$), mass ($[1.0, 5.0]$ kg), and lateral (linear) contact friction coefficient ($[0.8, 1.2]$). Box widths are scaled by 0.8 to roughly match the length of its diagonal with the diameter of its cylindrical counterpart. We sample sphere sizes according to the object height sampling range, downscaled by 0.75. The minimum distance between object centroids was set to 25 cm. We randomly generate between 4 and 6 objects per scene, subject to the constraints listed above, and resample if generated objects fail to meet our criteria. We limit the number of resampling trials to 50. As a result, some scenes may have fewer than the desired object count.

For stacking, we set the minimum width of the bottom object in the stack to be slightly thicker (9 cm) to avoid overly difficult tests of stacking onto a narrower object than self. We additionally enforce shape and color uniqueness between the task objects and surrounding objects to ensure that the task specification is unambiguous without providing language commands.